Measurement of Band-to-Band Registration of the NPP VIIRS Instrument from On-Orbit Data

James C. Tilton[1], Bin Tan[2] and Guoqing (Gary) Lin[2]
email contact: James.C.Tilton@nasa.gov
[1] Code 606, NASA GSFC,
[2] Science, Systems and Application, Inc., Code 619, NASA GSFC

Introduction

The NASA/NOAA Visible Infrared Imaging Radiometer Suite (VIIRS) instrument onboard the Suomi National Polar-orbiting Partnership (SNPP) satellite was launched on 28 October 2011. VIIRS has 5 imagery resolution bands (bands I1 to I5) with 32 detectors each, 16 moderate resolution bands (bands M1 to M16) and a panchromatic day-night band (DNB) with 16 detectors each. In this study we estimate the along-scan and along-track band-to-band registration (BBR) of each band versus the other bands from on-orbit data. We utilized Normalized Mutual Information (NMI) between shifted image band pairs to determine the amount of shift required for the best match between the image band pairs. Subpixel accuracy was obtained by utilizing bicubic interpolation.

Normalized Mutual Information

Referring to [1-3], we can compute the Normalized Mutual Information (NMI) between two images as follows:

$$NMI(X_f;X_s) = \frac{[H(X_f)+H(X_s)]}{H(X_f,X_s)} - 1$$

where X_f is the fixed image and X_s is the shifted image. $H(X_f)$ ($H(X_s)$) is the entropy of image X_f (X_s) and $H(X_f,X_s)$ is the joint entropy of the images X_f and X_s. The entropy of an image X is computed as follows:

$$H(X) = -\sum_{p>0} p \log p$$

where p is the probability density function (pdf) of image X.

The pdf of image X may be estimated from the histogram of an appropriately scaled and quantized image. According to [2], 8-bit quantization is usually sufficient. To avoid potential problems with outlier values, we apply a 3σ filter such that μ-3σ (the mean minus 3 times the standard deviation) corresponds to the value 1 and μ+3σ corresponds to the value 255. The values are rounded to the nearest integer value (value "0" is reserved as a "no data" mask).

Bicubic Interpolation

Our implementation of bicubic interpolation is based on K. Joy's [4] summary description of the Catmull-Rom Splines [5]. A cubic curve can be represented parametrically by the polynomial function:

$$P(t) = a_0 + a_1 t + a_2 t^2 + a_3 t^3$$

that has the first derivative (slope):

$$P'(t) = a_1 + 2a_2 t + 3a_3 t^2.$$

An interpolated curve for t in the range of 0 to 1 can be specified by setting the values of $P(0)$, $P(1)$, $P'(0)$ and $P'(1)$ and solving the resulting system of equations:

$$P(0) = a_0$$
$$P(1) = a_0 + a_1 + a_2 + a_3$$
$$P'(0) = a_1$$
$$P'(1) = a_1 + 2a_2 + 3a_3$$

To fit an interpolative curve passing through n+1 control points (P_0, P_1, …, P_n) we define the curve for the segment P_i to P_{i+1} by setting $P(0) = P_i$, $P(1) = P_{i+1}$, $P'(0) = (P_{i+1} - P_{i-1})/2$ and $P'(1) = (P_{i+2} - P_i)/2$. Several algebraic steps lead to the following matrix equation for the interpolative curve $P(t)$ for each line segment P_i to P_{i+1}:

$$P(t) = [1\ t\ t^2\ t^3] M \begin{bmatrix} P_{i-1} \\ P_i \\ P_{i+1} \\ P_{i+2} \end{bmatrix} \text{ where } M = \frac{1}{2}\begin{bmatrix} 0 & 2 & 0 & 0 \\ -1 & 0 & 1 & 0 \\ 2 & -5 & 4 & -1 \\ -1 & 3 & -3 & 1 \end{bmatrix}$$

The above cubic interpolation for a single dimensional curve is extended to a two dimensional image by first performing the cubic interpolation along the column dimension and then applying it along the row dimension.

Analysis Scheme

1. Selected four relatively cloud free NPP VIIRS data sets from differing geographic areas:

NPP VIIRS data set	Date	Location
A2012065.1835.P1_03110	March 5, 2012	Eastern United States
A2014176.1720.P1_03110	June 25, 2014	Eastern Canada
A2014176.1900.P1_03110	June 25, 2014	Central Canada
A2014192.0855.P1_03110	July 11, 2014	Northwestern Russia

2. For each data set and band combination, found the 100 "best" chips:

a. Scanned through each data set to find relatively cloud-free "chips" that were not entirely over water. For the I-bands the chips were 64 cols. by 32 rows, and for the M-bands the chips were 32 cols. by 16 rows.

b. For each chip selected in step 2, calculated the zero-shift NMI with the data bicubic interpolated to 4 times finer resolution. Saved a list of the location of chips with the 100 highest NMI values.

c. For the 100 "best" chips found in step 3, calculated the NMI with at various row and column shift locations with the data bicubic interpolated to 40 times finer resolution.

3. Looking across all four data sets, for each band combination and aggregation zone, selected the chips with the highest NMI value more than 0.15.

4. If fewer than 20 chips were found in step 3 for a band combination (and also aggregation zone in the along scan direction), the BBR analysis was terminated due to inadequate data. Otherwise the analysis continued.

5. For each band combination (and also aggregation zone for the along scan direction) computed the average BBR shift of the 20 chips with the highest NMI value. Also computed the standard deviation of these shifts. We also noted the minimum NMI value as a relative quality factor.

References

[1] A. A. Cole-Rhodes and P. K. Varshey, "Image registration using mutual information," in *Image Registration for Remote Sensing*, J. L. LeMoigne, N. S. Netanyahu and R. D. Eastman, Eds., pp. 131-149, 2011.
[2] J. P. Kern and M. S. Pattichis, "Robust multispectral image registration using mutual information models," *IEEE Trans. Geosci. Remote Sens.*, 45(5), pp. 1494-1505, 2007.
[3] C. Studholme, D. L. G. Hill and D. Hawkes, "An overlap invariant entropy measure of 3D medical image alignment," *Pattern Recognition*, 32(1), pp. 71-86, 1999.
[4] K. I. Joy, "Catmull-Rom Splines," *On-Line Geometric Modeling Notes*, (http://graphics.cs.ucdavis.edu/~joy/ecs278/ notes/Catmull-Rom-Spline.pdf, last accessed Aug. 5, 2015).
[5] E. Catmull and R. Rom, "A class of local interpolating splines," in R. E. Barnhill and R. F. Riesenfled (eds.), *Computer Aided Geometric Design*, Academic Press, New York, 1974.

Abridged Results

Largest BBR Offsets

Along Scan in 3x1 Aggregation Zone:

Fixed band	Shifted band	Minimum peak NMI	Mean*	Std. Dev.
M2	M13	0.28	0.0338	0.019
M3	I5	0.16	-0.0388	0.093
M12	I1	0.18	-0.0338	0.078
M6	I1	0.18	0.0713	0.124
M8	I1	0.19	0.0375	0.074
M8	I3	0.27	0.0375	0.056
M11	I1	0.20	0.0413	0.067
M11	I4	0.25	0.0525	0.067

Along Scan in 2x1 Aggregation Zone:

Fixed band	Shifted band	Minimum peak NMI	Mean*	Std. Dev.
M1	M6	0.19	-0.1113	0.115
M2	M6	0.20	-0.0975	0.116
M3	M6	0.22	-0.0575	0.122
M6	M13	0.25	0.0563	0.018
M8	M13	0.28	0.0500	0.020
M11	M13	0.32	0.0475	0.026
M5	I4	0.18	0.0538	0.078
M5	I5	0.17	0.0625	0.100

Along Scan in 1x1 Aggregation Zone:

Fixed band	Shifted band	Minimum peak NMI	Mean*	Std. Dev.
M3	M13	0.21	0.0825	0.053
M6	M12	0.18	0.0963	0.055
M8	M10	0.50	0.0613	0.017
M11	M12	0.30	0.0700	0.026
M12	I1	0.17	-0.0688	0.047
M12	I3	0.17	-0.0638	0.047
M12	I5	0.21	-0.0700	0.046
M13	I3	0.15	-0.1050	0.063
M13	I4	0.23	-0.0900	0.032
M13	I5	0.23	-0.0838	0.076
M2	I1	0.17	0.0625	0.077

*Negative means shift to west, positive means shift to east.

Along Track BBR Across Aggregation Zones:

Fixed band	Shifted band	Minimum peak NMI	Mean+	Std. Dev.
M14	I2	0.18	-0.0550	0.078
M15	I2	0.20	-0.0563	0.061
M15	I3	0.20	-0.0500	0.041
M16	I2	0.18	-0.0588	0.061
M6	I5	0.18	0.0725	0.101
M7	I5	0.18	0.0688	0.118
M13	I5	0.33	0.0613	0.052
M14	I2	0.18	-0.0550	0.078
I1	I5	0.28	0.0588	0.015
I2	I5	0.25	0.0588	0.025
I3	I5	0.32	0.0525	0.016

+Negative means shift to north, positive means shift to south.

Pre-launch BBR (vs. I1)

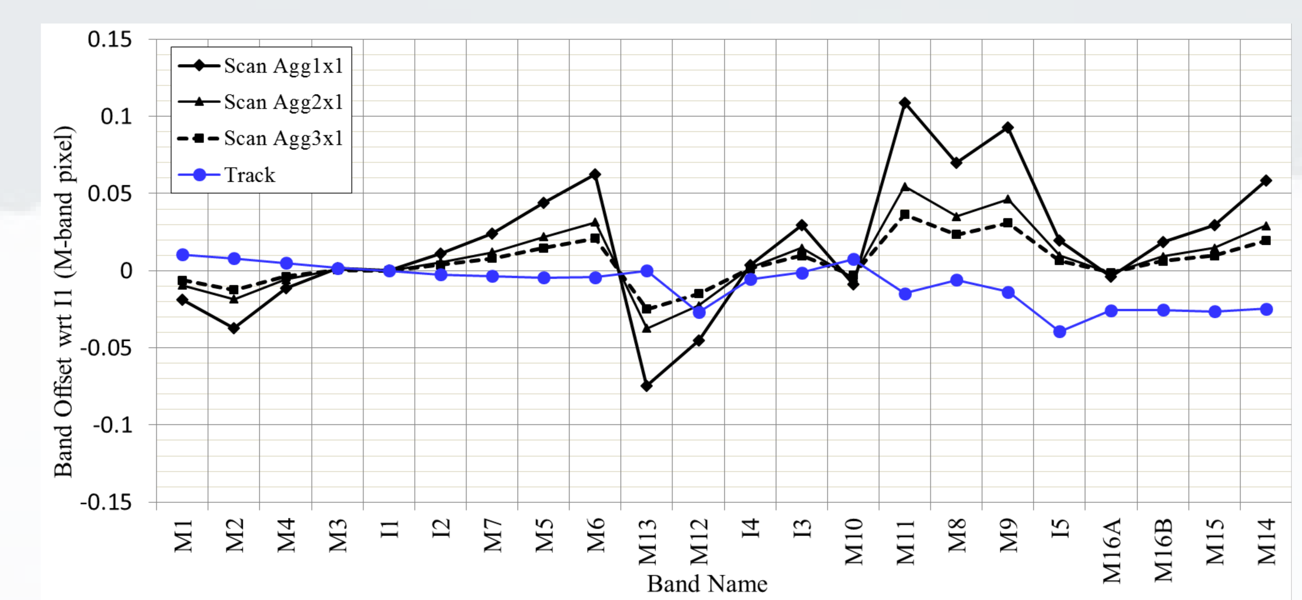

Discussion

The BBR values for band combinations not shown are lower than the shown cases. However, the BBR values for some band combinations could not be reliably measured. We considered finding at least 20 chips with peak NMI of at least 0.15 to be the minimum requirement for reliable measurement. Reliable measurements were found for most band combinations, with the main exception being band M9 versus any other band, where minimum peak NMI values greater than 0.15 were rarely found. Some other band combina-tions also had low minimum peak NMI values – mainly in the 1x1 aggregation zone. Full results are available in supplementary material.

A plot of pre-launch measurements of BBR versus band I1 is shown below. Many consistencies can be seen between these measurements and the on-orbit values. For example, band I5 is offset about 0.05 pixel from the other I-bands along track. Also band M6 is offset about 0.05 pixel from band M13 along scan in the 2x1 aggregation zone.

Some inconsistencies are also seen. A 0.045 pixel offset is seen between band I2 and I4 along scan in the 1x1 aggregation zone. But this may just be an inaccurate measurement since the minimum peak NMI is only 0.18.

NOTE: Measured BBR values between I-bands are fractions of I-band pixels. Other-wise the BBR values are fractions of M-band pixels.

Conclusions

Our approach for on-orbit measurement of the BBR of pairs of VIIRS bands has produced results that are largely consistent with the pre-launch measurements with maximum BBR offsets on the order of 0.1 pixel (10%).